CREEP ANALYSIS OF STRUCTURES USING A NEW EQUATION OF STATE TYPE CONSTITUTIVE RELATION

Virendra Kumar and Subrata Mukherjee

ERDA Report No: COO-2733-2

September 1975

Department of Theoretical and Applied Mechanics

Cornell University

Ithaca, N.Y. 14853

DISCLAIMER

ABSTRACT

A computational scheme is presented for the analysis of a certain class of problems involving creep of metals at elevated temperatures. The high temperature nonelastic behavior of materials is assumed to obey a new mechanical equation of state type constitutive relation recently proposed by Hart. As an illustration, the problem of creep of a closed-ended thick-walled cylinder under internal and external pressures is analysed employing the proposed computational scheme and Hart's equation of state approach. The results obtained are compared qualitatively with the results of classical strain hardening and time hardening theories of creep and the experimental results obtained earlier by other researchers. The proposed computational scheme is found to be very efficient from the view point of both computational time and effort. In regard to the equation of state approach, it is found that in addition to the general features of these classical creep theories, it is also capable of taking into account the effect of prior deformation history on subsequent creep behavior by simply specifying the initial distribution of a single state variable called hardness.

INTRODUCTION

The study of high temperature inelastic behavior of metals has received remarkable attention in the recent years. This growth of interest is mainly because of the vast technological applications of metals at elevated temperatures, especially in the nuclear power industry. In particular, great emphasis has been laid recently upon the development of constitutive relations for representing the time dependent inelastic behavior of metals which is highly nonlinear and hereditary in nature.

Various theories of creep, as described by Rabotnov [1] and Penny and Marriot [2], have been proposed in the past to represent this complex phenomenon of creep of metals. Of all these theories, strain hardening and time hardening laws are most commonly used at present for creep analysis of structures. Krempl [3,4] and Onat and Fardshisheh [5] have critically examined these classical theories and have concluded that they are incapable of representing all the salient features of high temperature deformation behavior of metals. For example, the strain hardening and the time hardening theories do not take into account the effect of prior deformation history on subsequent creep behavior, and both of them are incapable of representing a softening of the material which accompanies creep recovery. These theories are, therefore, inadequate for analysis of structures subjected to complex mechanical and thermal loadings at elevated temperatures.

Several modifications have been suggested to remedy such drawbacks of classical theories and to obtain a more faithful representation of the high temperature deformation behavior of metals. In this paper we shall concentrate on one such modern theory, namely the equation of

state approach due to Hart [6,7]. This theory involves the use of certain well defined state variables which depend upon the previous deformation history. A novel feature of this theory is its ability to incorporate in a simple way the difference between geometrically identical specimens with different initial deformation states, e.g. between annealed and cold worked specimens. The basic assumptions underlying the uniaxial constitutive relation for relatively steady loading have been justified experimentally for various metals and alloys by Hart, Li and their coworkers [6-15]. Also, uniaxial constant load creep experiments at 250° C have been performed by Ellis, Wire and Li [15] on 1100 Aluminum alloy specimens with different initial states. The results they have reported are in good agreement with theoretical predictions.

In regard to the application of Hart's theory to multiaxial states of stress situations, the present authors have recently analyzed the problem of creep of a thick-walled spherical shell under steady internal and external pressures [16]. The aim of this paper is twofold: (1) to present a general computational technique for solving boundary value problems arising in creep analysis of structures involving materials that obey either Hart's constitutive relation or classical strain or time hardening type creep theories, and (2) to analyze the problem of creep of a closed-ended thick-walled cylinder subjected to steady internal and external pressures using the proposed computational method and Hart's constitutive relation for the cylinder material. The results obtained are compared qualitatively with the time hardening results of Johnson [17] and Smith [18], and the strain hardening and experimental results of Taira [19, 20] and their coworkers. The main features of Hart's theory

are discussed and encouraging conclusions are drawn regarding the proposed computational scheme.

1. EQUATION OF STATE APPROACH DUE TO HART

In this section we shall outline the basic features of Hart's theory. A detailed description can be found in references [6, 7].

We shall concentrate our attention on the constitutive laws governing grain matrix deformation. For situations under consideration the contribution due to grain boundary sliding is neglible and is, therefore, not included in the present formulation of Hart's theory [7]. The accumulated total strain due to grain matrix deformation, ϵ^t, at any time can be decomposed into three components:

$$\epsilon^t = \epsilon^e + \epsilon^a + \epsilon^p \tag{1.1}$$

where ϵ^e is the elastic strain which is related to stress by Hooke's law; ϵ^a is the anelastic strain, a stored strain that is completely recoverable eventually upon unloading; and ϵ^p is the completely irrecoverable and path dependent permanent strain. The anelastic strain rate $\dot{\epsilon}^a$ is appreciable for relatively short times following abrupt changes of load and plays a very important role in cyclic loading. In case of relatively steady loading, however, we can use the transient free relationship in which $\dot{\epsilon}^a \approx 0$. In what follows we consider steady loading situations where we ignore the anelastic strain ϵ^a and consider only the elastic strain ϵ^e and permanent strain ϵ^p. It should be pointed out that ϵ^p represents the completely irrecoverable component of strain and includes the time independent as well as the time dependent plastic strains in a classical sense.

Relaxation tests have been performed by Hart, Li and their co-workers [8-15] on various metals and alloys at different temperatures. The results reported indicate that for samples of the same material at the same temperature but with different initial states, the log σ-log $\dot{\epsilon}^p$ curves form a one parameter family. Moreover, it is observed that in each case the family of curves can be generated by translation, without rotation, of a single master curve along a straight line. Thus, the family of curves obey on equation of state of the type

$$\sigma^* = y(\sigma, \dot{\epsilon}^p) \tag{1.2}$$

where σ^* is a well defined state variable, called hardness, which characterizes the present deformation state of the material. The hardness at certain time t depends upon the deformation history upto time t. Clearly, the hardness of a specimen increases with the amount of cold work and remains constant in a process where ϵ^p is held constant (as is approximately true in a relaxation test). Each relaxation curve is, therefore, regarded as a constant hardness curve.

The researchers mentioned above have also conducted a series of strain hardening tests at constant strain rates. It is found that the growth rate of hardness $\dot{\sigma}^*$ is a function of σ and σ^* only. Based upon these experiments Hart et al have obtained the following expressions for the equation of state and the kinetic law:

$$\dot{\epsilon}^p = A(\sigma, \sigma^*) = (\sigma^*/G)^m f \exp(-z/RT)\phi(\sigma/\sigma^*) \tag{1.3}$$

$$\dot{\sigma}^* = B(\sigma, \sigma^*) = \dot{\epsilon}^p \sigma^* \Gamma(\sigma, \sigma^*) \tag{1.4}$$

In the above f is an arbitrary coefficient with dimensions of frequency,

R is the gas constant, G is the isothermal modulus of rigidity and is a function of temperature, m is a material constant with a value between 3 and 8, z is a measure of thermal activation energy and is a function of temperature alone, T is temperature, and ϕ and Γ are measured functions of their arguments. The explicit forms of ϕ and Γ for 1100 Aluminum will be presented later. Note that there is no rate independent yeild stress and that the current values of σ, σ^* and T uniquely determine the permanent strain rate and the rate of growth of hardness.

The three dimensional generalization of the above constitutive relations is obtained in a straightforward manner. In keeping with concepts of incremental plasticity Hart [7] defines two invariants as follows:

$$\sigma = \sqrt{\frac{3}{2} s_{ij} s_{ij}} \tag{1.5}$$

$$\dot{\epsilon}^p = \sqrt{\frac{2}{3} \dot{\epsilon}^p_{ij} \dot{\epsilon}^p_{ij}} \tag{1.6}$$

where s_{ij} is the deviatoric stress tensor

$$s_{ij} = \sigma_{ij} - \frac{1}{3} \sigma_{kk} \delta_{ij} \tag{1.7}$$

In the above a repeated index implies summation over that index and δ_{ij} is the Kronecker delta.

It is now assumed that the invariants σ and $\dot{\epsilon}^p$ defined above by equations (1.5) and (1.6) are related to each other through the hardness σ^* according to equations (1.3) and (1.4). Finally, a flow rule relating the permanent strain rate to the deviatoric stress tensor is given by

$$\dot{\epsilon}^p_{ij} = \frac{3}{2}\left(\frac{\dot{\epsilon}^p}{\sigma}\right)s_{ij} \tag{1.8}$$

Equations (1.5)-(1.8) must reduce to (1.3)-(1.4) for the uniaxial case. In order to assure this, Hart's equations as given in [7] have been modified by proper numerical factors.

2. GENERAL METHOD OF ANALYSIS OF CREEP PROBLEMS

We now present a general computational method for analysis of creep problems. Although the scheme presented uses Hart's constitutive relation, we shall see later that its application to classical strain or time hardening type theories is straightforward. Since in this paper we are mainly concerned with relatively steady processes, the anelastic strain component ϵ^a is ignored. Thus, the total strain ϵ^t is the sum of elastic strain ϵ^e and permanent strain ϵ^p. The total strain rates $\dot{\epsilon}^t$ must satisfy the compatibility condition

$$\underset{\sim}{\nabla} \times \dot{\underset{\sim}{\epsilon}}^t \times \underset{\sim}{\nabla} \equiv \dot{\epsilon}^t_{ij,k\ell} + \dot{\epsilon}^t_{k\ell,ij} - \dot{\epsilon}^t_{ik,j\ell} - \dot{\epsilon}^t_{j\ell,ik} = 0 \tag{2.1}$$

where $\dot{\underset{\sim}{\epsilon}}$ is the strain rate tensor with cartesian components $\dot{\epsilon}_{ij}$ and $\underset{\sim}{\nabla}$ is the gradient operator defined as

$$\underset{\sim}{\nabla} = \underset{\sim}{e}_1 \frac{\partial}{\partial x_1} + \underset{\sim}{e}_2 \frac{\partial}{\partial x_2} + \underset{\sim}{e}_3 \frac{\partial}{\partial x_3}$$

$\underset{\sim}{e}_m$ being the triad of orthogonal unit vectors. Since $\dot{\underset{\sim}{\epsilon}}^t = \dot{\underset{\sim}{\epsilon}}^e + \dot{\underset{\sim}{\epsilon}}^p$, the compatibility equation (2.1) can be written as

$$\underset{\sim}{\nabla} \times \dot{\underset{\sim}{\epsilon}}^e \times \underset{\sim}{\nabla} = -\underset{\sim}{\nabla} \times \dot{\underset{\sim}{\epsilon}}^p \times \underset{\sim}{\nabla} \tag{2.2}$$

The elastic strain rates are related to stress rates by Hooke's law

$$\dot{\underset{\sim}{\epsilon}}^{e} = \frac{1}{2G}\left(\dot{\underset{\sim}{\sigma}} - \frac{\mu}{1+\mu}\dot{\Theta}\underset{\sim}{I}\right) \tag{2.3}$$

and the permanent strain rates to stresses by Hart's constitutive relation

$$\dot{\underset{\sim}{\epsilon}}^{p} = \frac{3}{2}\frac{A(\sigma,\sigma^{*})}{\sigma}\underset{\sim}{s} \tag{2.4}$$

where G and μ are the shear modulus and Poisson's ratio respectively, $\underset{\sim}{I}$ is the unit tensor, $\underset{\sim}{\sigma}$ is the stress tensor with cartesian components σ_{ij}, and $\Theta = \text{tr}\ \underset{\sim}{\sigma} = \sigma_{kk}$. Substitution of (2.3) and (2.4) into (2.2) yields

$$\underset{\sim}{\nabla} \times \left[\frac{1}{2G}\left(\dot{\underset{\sim}{\sigma}} - \frac{\mu}{1+\mu}\dot{\Theta}\underset{\sim}{I}\right)\right] \times \underset{\sim}{\nabla} = -\underset{\sim}{\nabla} \times \left[\frac{3}{2}\frac{A(\sigma,\sigma^{*})}{\sigma}\underset{\sim}{s}\right] \times \underset{\sim}{\nabla} \tag{2.5}$$

The stress rates must satisfy the equilibrium equation

$$\underset{\sim}{\nabla}\cdot\dot{\underset{\sim}{\sigma}} = -\dot{\underset{\sim}{F}} \tag{2.6}$$

where $\underset{\sim}{F}$ is the given body force per unit volume. In (2.6) the inertial terms are neglected because we are considering only quasi-steady processes. Finally, the hardness evolves with time according to the kinetic law

$$\dot{\sigma}^{*} = B(\sigma,\sigma^{*}) \tag{2.7}$$

The boundary condition is

$$\dot{\underset{\sim}{\sigma}}\cdot\underset{\sim}{n} = \dot{\underset{\sim}{\tau}} \tag{2.8}$$

where $\underset{\sim}{n}$ is outward unit normal to the boundary and $\underset{\sim}{\tau}$ is the prescribed surface traction vector.

The initial deformation state of the solid should be specified by prescribing the hardness $\sigma^{*}(x_i,0)$. The deformation history prior

to time $t = 0$ is completely taken into account by specifying $\sigma^*(x_i,0)$ and the initial permanent strains are taken to be zero. (In most cases the initial hardness distribution would be uniform throughout the material, i.e. $\sigma^*(x_i,0) = \text{constant}$. But nonhomogeneous initial hardness may be introduced during fabrication of the structure such as due to machining and forming processes). Since $\underset{\sim}{\epsilon}^p = 0$ at $t = 0$, the stresses and strains at time $t = 0$ are given by the corresponding elastic solution of the problem. Thus, the initial conditions are

$$\underset{\sim}{\sigma}(x_i,0) = \underset{\sim}{\sigma}^o(x_i) \quad , \quad \underset{\sim}{\epsilon}^e(x_i,0) = \underset{\sim}{\epsilon}^o(x_i) \quad , \quad \underset{\sim}{\epsilon}^p(x_i,0) = 0 \quad , \quad \sigma^*(x_i,0) = \sigma_o^*(x_i) \tag{2.9}$$

where $\underset{\sim}{\sigma}^o(x_i)$ and $\underset{\sim}{\epsilon}^o(x_i)$ correspond to the elastic solution at $t = 0$. In other words, $\underset{\sim}{\sigma}^o$ and $\underset{\sim}{\epsilon}^o$ are obtained by solving the following system of equations:

$$\underset{\sim}{\epsilon}^o = \frac{1}{2G}\left(\underset{\sim}{\sigma}^o - \frac{\mu}{1+\mu}\,\theta^o \underset{\sim}{I}\right) \tag{2.10}$$

$$\underset{\sim}{\nabla} \times \left[\frac{1}{2G}\left(\underset{\sim}{\sigma}^o - \frac{\mu}{1+\mu}\,\theta^o \underset{\sim}{I}\right)\right] \times \underset{\sim}{\nabla} = 0 \tag{2.11}$$

$$\underset{\sim}{\nabla} \cdot \underset{\sim}{\sigma}^o = -\underset{\sim}{F}^o \tag{2.12}$$

$$\underset{\sim}{\sigma}^o \cdot \underset{\sim}{n} = \underset{\sim}{\tau}^o \tag{2.13}$$

Here $\underset{\sim}{F}^o$ is the body force per unit volume at $t = 0$.

The proposed computational scheme proceeds as follows: the initial stresses and strains are first obtained by solving the elasticity problem governed by equations (2.10)-(2.13). Once $\underset{\sim}{\sigma}^o$ and σ_o^* are known,

the stress and hardness rates at $t = 0$ are obtained by solving the set of linear, inhomogeneous, partial differential equations (2.5)-(2.7) subject to the boundary condition (2.8). The stresses and hardness are then obtained at a new time Δt by using, for example, the Euler's method $\underset{\sim}{\sigma}|_{\Delta t} = \underset{\sim}{\sigma}^{o} + \dot{\underset{\sim}{\sigma}}|_{t=o} \times \Delta t$ and $\sigma^{*}|_{\Delta t} = \sigma_{o}^{*} + \dot{\sigma}^{*}|_{t=o} \times \Delta t$ (higher order integration methods such as the fourth-order Runge-Kutta method may also be used to obtain $\underset{\sim}{\sigma}|_{\Delta t}$ and $\sigma^{*}|_{\Delta t}$). These new stresses and hardness are now used to obtain the rates at time Δt and so on, and the process continued upto the desired final time. Thus, knowing the stress and hardness at time t, the rates at time t are obtained by solving the boundary value problem (2.5)-(2.8), and then the stresses and hardness at time $t + \Delta t$ are obtained by using $\underset{\sim}{\sigma}|_{t+\Delta t} = \underset{\sim}{\sigma}|_{t} + \dot{\underset{\sim}{\sigma}}|_{t} \times \Delta t$ and $\sigma^{*}|_{t+\Delta t} = \sigma^{*}|_{t} + \dot{\sigma}^{*}|_{t} \times \Delta t$ or some other suitable integration scheme. It should be pointed out that the boundary value problem (2.5)-(2.8) can be solved analytically only for a few cases. For complicated problems, one may have to use finite difference or finite element methods to solve the boundary value problem (2.10)-(2.13) for initial stresses and the boundary value problem (2.5)-(2.8) for stress and hardness rates. The strain history is obtained by using equations (2.3) and (2.4). Choice of time step Δt is found to be very crucial in the computation. Initial time steps must be small because the rates are rather high in the beginning.

If classical creep theories are used, equation (2.4) should be suitabably modified and equation (2.7) dropped. For example, equation (2.4) should be replaced by $\dot{\underset{\sim}{\epsilon}}^{p} = \frac{3}{2} \frac{g_s(\sigma, \epsilon^p)}{\sigma} \underset{\sim}{s}$ for strain hardening theory, and by $\dot{\underset{\sim}{\epsilon}}^{p} = \frac{3}{2} \frac{g_t(\sigma, t)}{\sigma} \underset{\sim}{s}$ for time hardening theory.

3. GOVERNING EQUATIONS FOR THICK-WALLED CYLINDER

Let us now consider the equations governing the creep behavior of a closed-ended thick-walled cylinder subjected to constant internal and external pressures as shown in Fig. 1. Because of cylindrical symmetry, the tangential dispalcement component u_θ is zero. The end effects are neglected and the solution is assumed to be valid sufficiently far from the ends. Therefore, the radial displacement component u_r is a function of the radius r and time t only. The kinematic equations for non-vanishing strains are

$$\epsilon_r^e + \epsilon_r^p = \frac{\partial u_r}{\partial r} \tag{3.1}$$

$$\epsilon_\theta^e + \epsilon_\theta^p = \frac{u_r}{r} \tag{3.2}$$

$$\epsilon_z^e + \epsilon_z^p = \frac{\partial u_z}{\partial z} \tag{3.3}$$

where u_z is the axial component of the displacement. The equilibrium equations in radial and axial directions are

$$\frac{\partial \sigma_r}{\partial r} - \frac{1}{r}(\sigma_\theta - \sigma_r) = 0 \tag{3.4}$$

$$\int_a^b \sigma_z 2\pi r \, dr = \pi(a^2 p - b^2 q) \tag{3.5}$$

where a and b are internal and external radii of the cylinder and p and q are the internal and external pressures respectively. The elastic strain components are governed by Hooke's law

$$\epsilon_r^e = \frac{1}{2G}[\sigma_r - \frac{\mu}{1+\mu}(\sigma_r+\sigma_\theta+\sigma_z)] \tag{3.6}$$

$$\epsilon_\theta^e = \frac{1}{2G}[\sigma_\theta - \frac{\mu}{1+\mu}(\sigma_r+\sigma_\theta+\sigma_z)] \tag{3.7}$$

$$\epsilon_z^e = \frac{1}{2G}[\sigma_z - \frac{\mu}{1+\mu}(\sigma_r+\sigma_\theta+\sigma_z)] \tag{3.8}$$

The permanent strain rates are governed by the flow rule

$$\dot{\epsilon}_r^p = \frac{3}{2}(\frac{\dot{\epsilon}^p}{\sigma})s_r = \frac{1}{2}(\frac{\dot{\epsilon}^p}{\sigma})(2\sigma_r-\sigma_\theta-\sigma_z) \tag{3.9}$$

$$\dot{\epsilon}_\theta^p = \frac{3}{2}(\frac{\dot{\epsilon}^p}{\sigma})s_\theta = \frac{1}{2}(\frac{\dot{\epsilon}^p}{\sigma})(2\sigma_\theta-\sigma_r-\sigma_z) \tag{3.10}$$

$$\dot{\epsilon}_z^p = \frac{3}{2}(\frac{\dot{\epsilon}^p}{\sigma})s_z = \frac{1}{2}(\frac{\dot{\epsilon}^p}{\sigma})(2\sigma_z-\sigma_r-\sigma_\theta) \tag{3.11}$$

At this point we assume that there is no creep in the axial direction, i.e.

$$\dot{\epsilon}_z^p = 0 \tag{3.12}$$

Johnson [17], Taira [19, 20] and their coworkers have supported this assumption by arguing that $\dot{\epsilon}_z^p$ is so small compared to $\dot{\epsilon}_r^p$ and $\dot{\epsilon}_\theta^p$ that it can be neglected for all practical purposes. Smith [18], however, has taken axial creep into account and has analyzed the problem using a complicated finite difference procedure. His results also indicate that $\dot{\epsilon}_z^p$ is negligible compared to $\dot{\epsilon}_r^p$ and $\dot{\epsilon}_\theta^p$. Note that equation (3.12) implies that plane cross sections do not remain plane and the compatibility condition in the z direction is not satisfied just like for the plane stress case of classical elasticity. Equation (3.12) together with (3.11) gives

$$\sigma_z = (\sigma_r+\sigma_\theta)/2 \tag{3.13}$$

It is shown in Appendix A that the above relation for σ_z satisfies the equilibrium equation in the axial direction (3.5).

The invariants σ and $\dot{\epsilon}^p$ now become

$$\sigma = \sqrt{3}(\sigma_\theta-\sigma_r)/2 = -\sqrt{3}\, s_r \tag{3.14}$$

$$\dot{\epsilon}^p = -2\dot{\epsilon}^p_r/\sqrt{3} \tag{3.15}$$

Equation (3.15) follows from the condition of incompressibility of permanent strains, $\dot{\epsilon}^p_r + \dot{\epsilon}^p_\theta = 0$. Note that σ and $\dot{\epsilon}^p$ are, by definition, positive quantities. The boundary conditions are

$$\sigma_r(a,t) = -p \quad , \quad \sigma_r(b,t) = -q \tag{3.16}$$

and the initial conditions, with $\epsilon^p_r(r,0) = \epsilon^p_\theta(r,0) = 0$, are given by the Lame's solution to the corresponding elastic problem. The initial stress distributions, therefore, are

$$\sigma_r(r,0) = \frac{1}{b^2-a^2}\left[a^2p-b^2q-\frac{a^2b^2}{r^2}(p-q)\right] \tag{3.17}$$

$$\sigma_\theta(r,0) = \frac{1}{b^2-a^2}\left[a^2p-b^2q+\frac{a^2b^2}{r^2}(p-q)\right] \tag{3.18}$$

$$\sigma_z(r,0) = [\sigma_r(r,0)+\sigma_\theta(r,0)]/2 = (a^2p-b^2q)/(b^2-a^2) \tag{3.19}$$

Finally, the initial distribution of hardness must be specified

$$\sigma^*(r,0) = \sigma^*_o(r) \tag{3.20}$$

4. METHOD OF SOLUTION TO THE CYLINDER PROBLEM

The equations presented in the preceeding section can be solved numerically to obtain the desired solution. However, if these equations are used in their present form, the computational procedure is complex and involves solving a succession of nonlinear two-point boundary value problems at each time. Using the ideas outlined in Section 2, we present here a scheme for manipulating these equations so that they reduce to an initial value problem in time at each radius r. Since, in general, solutions of initial value problems are computationally much simpler than of two-point boundary value problems, this method results in a substantial saving in computational time and effort.

Using equations (3.1) and (3.2) and separating the elastic and permanent components, the compatibility equation in terms of strain rates can be written as

$$\dot{\epsilon}_r^e - \dot{\epsilon}_\theta^e - r\frac{\partial \dot{\epsilon}_\theta^e}{\partial r} = -\dot{\epsilon}_r^p + \dot{\epsilon}_\theta^p + r\frac{\partial \dot{\epsilon}_\theta^p}{\partial r} \tag{4.1}$$

Noting that $s_\theta = -s_r$, the equilibrium equation (3.4) can be rewritten in terms of rates of the mean stress $\sigma_m = (\sigma_r+\sigma_\theta+\sigma_z)/3$ and the deviatoric stresses as

$$\frac{\partial \dot{\sigma}_m}{\partial r} = -\frac{\partial \dot{s}_r}{\partial r} - \frac{2}{r}\dot{s}_r \tag{4.2}$$

We now replace the elastic strain rates in (4.1) in terms of $\dot{s}_r$ and $\dot{\sigma}_m$ using (3.6)-(3.8), and use (4.2) to eliminate $\dot{\sigma}_m$ in favor of $\dot{s}_r$. The right hand side of (4.1) is written in compact form by using the incompressibility relation $\dot{\epsilon}_\theta^p = -\dot{\epsilon}_r^p$. This gives

$$\frac{(2-\mu)}{2G(1+\mu)} \frac{1}{r} \frac{\partial}{\partial r}(r^2 \dot{s}_r) = -\frac{1}{r} \frac{\partial}{\partial r}(r^2 \dot{\epsilon}^p_r) \tag{4.3}$$

which can be integrated to yield

$$\dot{s}_r + \alpha \dot{\epsilon}^p_r = H(t)/r^2 \tag{4.4}$$

where

$$\alpha = 2G(1+\mu)/(2-\mu)$$

and $H(t)$ is an as yet undetermined function of time. This function can be obtained by using the equilibrium equation (4.2). Using $\dot{\sigma}_r = \dot{s}_r + \dot{\sigma}_m$, and integrating (4.2) gives

$$(\dot{\sigma}_r)_{r=b} - (\dot{\sigma}_r)_{r=a} + 2\int_a^b \frac{\dot{s}_r}{r}\, dr = 0 \tag{4.1}$$

which, for constant internal and external pressures, simplifies to

$$\int_a^b \frac{\dot{s}_r}{r}\, dr = 0 \tag{4.6}$$

Using (4.6) in (4.4), we can solve for $H(t)$. Resubstituting for $H(t)$ into (4.4) gives

$$\dot{s}_r = -\alpha \left[\dot{\epsilon}^p_r - \frac{2a^2b^2}{(b^2-a^2)} \frac{1}{r^2} \int_a^b \frac{\dot{\epsilon}^p_r}{r}\, dr \right] \tag{4.7}$$

So far we have used all the equations except those relating the permanent strain rates to the stresses (3.9-3.12, 1.3) and the kinetic law (1.4). Using the equation of state (1.3) together with the equations (3.14) and (3.15) for the invariants σ and $\dot{\epsilon}^p$, we obtain

$$\dot{\epsilon}_r^p = -\frac{\sqrt{3}}{2}\left(\frac{\sigma^*}{G}\right)^m f \exp(-z/RT)\phi\left(-\frac{\sqrt{3}\, s_r}{\sigma^*}\right) \tag{4.8}$$

Substituting (4.8) into (4.7) gives us an equation for $\dot{s}_r$ as a function of s_r and σ^*. In the kinetic law (1.4), we substitute for $\dot{\epsilon}^p$ in terms of s_r and σ^* using (3.14) to obtain an equation for $\dot{\sigma}^*$ in terms of s_r and σ^*. Thus, our final equations for $\dot{s}_r$ and $\dot{\sigma}^*$ assume the following forms

$$\dot{s}_r = \alpha\frac{\sqrt{3}}{2}\left[\left(\frac{\sigma^*}{G}\right)^m f \exp\left(-\frac{z}{RT}\right)\phi\left(-\frac{\sqrt{3}\, s_r}{\sigma^*}\right) - \frac{2a^2b^2}{(b^2-a^2)}\frac{1}{r^2}\int_a^b \frac{1}{r}\left(\frac{\sigma^*}{G}\right)^m f \exp\left(-\frac{z}{RT}\right)\phi\left(-\frac{\sqrt{3}\, s_r}{\sigma^*}\right)dr\right] \tag{4.9}$$

$$\dot{\sigma}^* = \left(\frac{\sigma^*}{G}\right)^m f \exp\left(-\frac{z}{RT}\right)\phi\left(-\frac{\sqrt{3}\, s_r}{\sigma^*}\right)\sigma^*\Gamma(-\sqrt{3}s_r, \sigma^*) \tag{4.10}$$

The initial condition for s_r is given by

$$s_r(r,0) = -[\sigma_\theta(r,0)-\sigma_r(r,0)]/2 \tag{4.11}$$

where $\sigma_r(r,0)$, $\sigma_\theta(r,0)$ are given by (3.17) and (3.18) respectively. The initial hardness distribution $\sigma^*(r,0)$ is given by (3.20).

Given the initial stress and hardness disturbution, equations (4.9) and (4.10) are used to calculate the rates $\dot{s}_r(r,0)$, $\dot{\sigma}^*(r,0)$. These rates are then used to obtain $s_r(r,\Delta t)$, $\sigma^*(r,\Delta t)$ after a small time interval Δt by using a suitable integration scheme. These, in turn are resubstituted into (4.9), (4.10) to obtain $\dot{s}_r(r,\Delta t)$, $\dot{\sigma}^*(r,\Delta t)$ and the process continued as long as desired. Once $s_r(r,t)$, $\sigma^*(r,t)$ are

known, the complete stress history is obtained from the following equations

$$\sigma_r(r,t) = -2\int_a^r \frac{s_r(\eta,t)}{\eta}\, d\eta - p \tag{4.12}$$

$$\sigma_\theta(r,t) = -2s_r(r,t) + \sigma_r(r,t) \tag{4.13}$$

$$\sigma_z(r,t) = [\sigma_r(r,t)+\sigma_\theta(r,t)]/2 \tag{4.14}$$

Equation (4.12) follows from the equilibrium equation written in terms of s_r and σ_m (see (4.2)) and the boundary condition (3.16), The strain history can now be obtained using equations (1.3), (3.6)-(3.12).

We now introduce the following nondimensionalization:

$$\bar{\sigma}_r = \sigma_r/p \ , \ \bar{\sigma}_\theta = \sigma_\theta/p \ , \ \bar{\sigma}_z = \sigma_z/p \ , \ \bar{\bar{\sigma}}^* = \bar{\sigma}^*/p \ ,$$

$$\bar{s}_r = s_r/p \ , \ \bar{s}_\theta = s_\theta/p \ , \ \bar{\sigma} = \sigma/p \ , \ \bar{q} = q/p \ ,$$

$$\bar{\alpha} = \alpha/p \ , \ \bar{G} = G/p \ , \ \xi = r/a \ , \ \kappa = b/a \tag{4.15}$$

Using these nondimensionalized variables, the equations (4.9), (4.10), (3.17)-(3.20) and (4.12)-(4.14) become

$$\dot{\bar{s}}_r = \frac{\bar{\alpha}\sqrt{3}}{2}\left[\left(\frac{\bar{\bar{\sigma}}^*}{\bar{G}}\right)^m f \exp\left(-\frac{Z}{RT}\right)\phi\left(-\frac{\sqrt{3}\,\bar{s}_r}{\bar{\bar{\sigma}}^*}\right) - \frac{2\kappa^2}{(\kappa^2-1)}\,\frac{1}{\xi^2}\int_1^\kappa \frac{1}{\xi}\left(\frac{\bar{\bar{\sigma}}^*}{\bar{G}}\right)^m f \exp\left(-\frac{z}{RT}\right)\phi\left(-\frac{\sqrt{3}\,\bar{s}_r}{\bar{\bar{\sigma}}^*}\right)d\xi\right] \tag{4.16}$$

$$\dot{\bar{\bar{\sigma}}}^* = \left(\frac{\bar{\bar{\sigma}}^*}{\bar{G}}\right)^m f \exp\left(-\frac{z}{RT}\right)\phi\left(-\frac{\sqrt{3}\,\bar{s}_r}{\bar{\bar{\sigma}}^*}\right)\bar{\bar{\sigma}}^*\Gamma(-\sqrt{3}p\bar{s}_r, p\bar{\bar{\sigma}}^*) \tag{4.17}$$

$$\bar{\sigma}_r(\xi,0) = \frac{1}{\kappa^2-1}\left[1-\kappa^2\bar{q}-\frac{\kappa^2}{\xi^2}(1-\bar{q})\right] \tag{4.18}$$

$$\bar{\sigma}_\theta(\xi,0) = \frac{1}{\kappa^2-1}\left[1-\kappa^2\bar{q}+\frac{\kappa^2}{\xi^2}(1-\bar{q})\right] \tag{4.19}$$

$$\bar{\sigma}_z(\xi,0) = (1-\kappa^2\bar{q})/(\kappa^2-1) \tag{4.20}$$

$$\bar{\sigma}^*(\xi,0) = \bar{\sigma}_o^*(\xi) \tag{4.21}$$

$$\bar{\sigma}_r(\xi,t) = -2\int_1^\xi \frac{\bar{s}_r(\eta,t)}{\eta}\,d\eta - 1 \tag{4.22}$$

$$\bar{\sigma}_\theta(\xi,t) = -2\bar{s}_r(\xi,t) + \bar{\sigma}_r(\xi,t) \tag{4.23}$$

$$\bar{\sigma}_z(\xi,t) = [\bar{\sigma}_r(\xi,t)+\bar{\sigma}_\theta(\xi,t)]/2 \tag{4.24}$$

Let us next consider the situation when a large amount of plastic strain has developed, i.e. $|\epsilon_{ij}^p| \gg |\epsilon_{ij}^e|$ (we are assuming here that the strains are still within the domain of infinitesimal strain theory). Then it may be plausible to assume that the hardness σ^* has reached the saturation limit and changes very slowly with time so that it can be regarded as stationary for all practical purposes. Under these conditions, the stresses can be assumed to have reached a stationary state where they no longer change in time. The procedure for calculating the stationary stresses $\sigma_r^s(r)$, $\sigma_\theta^s(r)$, $\sigma_z^s(r)$ is given in Appendix B.

5. BEHAVIOR of 1100 ALUMINIUM ALLOY

The above analysis has been carried out in terms of the functions $\phi(\sigma/\sigma^*)$ and $\Gamma(\sigma/\sigma^*)$, the explicit forms of which depends upon the material of interest. As an illustration, we shall consider a cylinder of 1100 Aluminum alloy at 250°C. Ellis, Wire and Li [15] have found experimentally that the equation of state (1.3) and the kinetic law (1.4) for 1100 Al. alloy at 250°C can be represented by the equations

$$\dot{\epsilon}^p = \left(\frac{\sigma}{D}\right)^{m} \left(\ln \frac{\sigma^*}{\sigma}\right)^{-1/\lambda} \tag{5.1}$$

$$\dot{\sigma}^* = \left(\frac{\sigma}{D}\right)^{m} \left(\ln \frac{\sigma^*}{\sigma}\right)^{-1/\lambda} \sigma^* \Lambda \frac{\sigma^{\delta}}{\sigma^{*\beta}} \tag{5.2}$$

where $m = 5$, $\lambda = .11$, $\delta = 7.82$, $\beta = 12.5$,

$$D = 10^{5.03}\text{psi}(\text{sec})^{1/m} \quad \text{at} \quad 250°C$$

and

$$\Lambda = 1.17 \times 10^{20}(\text{psi})^{\beta-\delta}.$$

In these equations, σ and σ^* are in units of psi and t is in seconds. Note that

$$D = \frac{G}{[f \exp(-z/RT)]^{1/m}}$$

and that (5.1), (5.2) are valid for temperatures $\geq$ about 1/3 of the melting temperature, for which $\sigma^* > \sigma$. The shear modulus and Poisson's ratio for this material at 250°C are [21]

$$G = 3.234 \times 10^{6}\text{psi}, \quad \mu = 0.358$$

The equations (4.16) and (4.17) for 1100 Al. alloy now become

$$\dot{\bar{s}}_r = \frac{\bar{\alpha}\sqrt{3}}{2}\left[\left(\frac{\bar{\sigma}^*}{\bar{D}}\right)^m \left(\ln\left(-\frac{\bar{\sigma}^*}{\sqrt{3}\,\bar{s}_r}\right)\right)^{-1/\lambda} - \frac{2\kappa^2}{(\kappa^2-1)}\frac{1}{\xi^2}\int_1^{\kappa}\frac{1}{\xi}\left(\frac{\bar{\sigma}^*}{\bar{D}}\right)^m \left(\ln\left(-\frac{\bar{\sigma}^*}{\sqrt{3}\,\bar{s}_r}\right)\right)^{-1/\lambda} d\xi\right] \tag{5.3}$$

$$\dot{\bar{\sigma}}^* = \left(\frac{\bar{\sigma}^*}{\bar{D}}\right)^m \left(\ln\left(-\frac{\bar{\sigma}^*}{\sqrt{3}\,\bar{s}_r}\right)\right)^{-1/\lambda} \bar{\Lambda}\,\frac{(-\sqrt{3}\,\bar{s}_r)^{\delta}}{\bar{\sigma}^{*\beta-1}} \tag{5.4}$$

where $\bar{D} = D/p$ and $\bar{\Lambda} = \Lambda p^{\delta-\beta}$. The corresponding equations for the stationary state are given in Appendix B.

6. RESULTS AND DISCUSSIONS

Numerical calculations have been carried out for an 1100 Al. cylinder at 250°C with κ, the ratio of external and internal radii, equal to 2. The internal pressure is taken to be 1250 psi (except for curve I, Fig. 6), the external pressure zero, and several distributions of the initial hardness $\sigma_o^*(r)$ are considered.

The Runge-Kutta method of order four has been used for solving the system of equations (5.3) and (5.4) subject to the initial conditions (4.18)-(4.21). The integrals in (5.3) and (4.22) have been evaluated using Simpson's rule. For numerical purposes, the nondimensionalized shell thickness, κ-1, has been divided into 20 equal segments. The computations have been carried out on an IBM 370/168 computer.

Figs. 2,3 and 4 show the distribution of radial, circumferential and axial stresses across a cross-section normal to the cylinder axis. The variation of stresses is qualitatively similar to that obtained from

time hardening [17, 18] and strain hardening [19, 20] theories. It is observed that stress redistribution occurs during creep and the stresses tend toward a stationary state. The corresponding stress distribution curves for 1100 Aluminum Alloy using time and strain hardening theories could not be obtained because the parameters for this material required for applying these classical theories are not available. Thus, a quantitative comparison with results from classical theories was not possible.

The effect of initial state, i.e. initial hardness distribution, is shown in Figs. 2-4 by assuming two different initial values of uniform hardness. The initial hardness level characterizes the initial state of a specimen and is determined by its previous mechanical and thermal history. The former is 10% cold worked while the latter is lightly cold worked. We observe, as expected, that the hoop and axial stresses (Figs. 3, 4) in the softer cylinder relax faster than in the hardened cylinder. The ability to easily distinguish between different initial states is a novel feature of the equation of state approach.

The initial hardness distribution for the cases shown in Figs. 2-4 is taken to be uniform and it is found that the cylinder hardens with creep. However, the change in hardness is too small to be evident within plotting accuracy. This is a consequence of the fact that the initial hardness level in these cases is such that $\dot{\bar{\sigma}}^*$, from equation (5.2), is very small. It is concievable that a sphere made of some other material, with the same level of initial hardness, will harden appreciably as it creeps.

In order to see how the theory predicts hardening with creep we consider next a cylinder which is hardened inside and soft outside. In particular, we choose the distribution $\bar{\sigma}_o^*(\xi) = 1.5\ \bar{\sigma}(\xi,0)$. The results

are shown in Fig. 5. We observe that the softer portions of the cylinder harden much more than the initially hardened inside.

Fig. 6 shows the creep of the inner radius with time for five different cases. For the same pressure (1250 psi) the amount of creep decreases with increase in level of uniform initial hardness (III, IV, V). A cylinder with variable initial hardness (II) given by $\bar{\sigma}_o^*(\xi) = 1.5\ \bar{\sigma}(\xi,0)$ is much less resistant to creep than a corresponding uniformly hardened cylinder (IV). Finally, a comparison of (I) with (V) shows the highly nonlinear effect of internal pressure. Similar results were obtained by the present authors for the creep of a sphere [16] and by Li et al for uniaxial creep [15].

Choice of time step is very crucial in the computation and variable time steps are necessary. The initial time steps must be small because the rate of creep is higher in the beginning. The computational scheme used is very efficient. Typical computing time for the results presented in Figs. 2-4, for example, is approximately 20 seconds on an IBM 370/168.

7. CONCLUSIONS

The equation of state approach due to Hart has been previously verified experimentally for relatively steady, uniaxial loading for various metals and alloys. An important new feature of this theory is that the effect of prior deformation history on subsequent creep behavior of the material can be taken into account by simply specifying the initial distribution of a single space variable called hardness.

In this paper we have presented an efficient computational scheme for analysis of creep of materials obeying classical or equation of

state type constitutive laws. As an example, the problem of creep of a closed-ended thick cylinder under steady internal and external pressures has been solved using Hart's Constitutive laws. Results for various specified levels of initial hardness are presented. It is found that the results are qualitatively similar to those obtained from classical theories, and, as expected, hardened cylinders resist creep more efficiently than softer ones. It is anticipated that an extended version of this theory including the anelastic strain component will provide a better model than the presently available classical theories for inelastic analysis of structures subjected to cyclic loading at elevated temperatures.

ACKNOWLEDGEMENTS

This research was supported by Contract No. E(11-1)-2733 of the Energy Research and Development Administration, Washington, D.C., with Cornell University, Ithaca, N.Y. Sincere thanks are expressed to Dr. E.W. Hart of General Electric Corporation, Schenectady, New York and Professors C.Y. Li and R.H. Lance of the Cornell Engineering School for valuable discussions.

APPENDIX A

The equilibrium equation (3.4) can be written as

$$\sigma_\theta - \sigma_r = r \frac{\partial \sigma_r}{\partial r}$$

which gives

$$\sigma_\theta + \sigma_r = \frac{1}{r} \frac{\partial}{\partial r}(r^2 \sigma_r)$$

Using the equation (3.13) that $\sigma_z = (\sigma_r + \sigma_\theta)/2$, the above relation and the boundary conditions (3.16) we get

$$2\pi \int_a^b r\sigma_z dr = \pi \int_a^b r(\sigma_r + \sigma_\theta) dr$$

$$= \pi \int_a^b \frac{\partial}{\partial r}(r^2 \sigma_r) dr$$

$$= \pi(pa^2 - qb^2)$$

thus the condition of axial equilibrium, namely equation (3.5), is satisfied.

APPENDIX B

When the elastic strains are negligible compared to permanent strains, the compatibility equation (4.1) together with the relation $\dot{\epsilon}_\theta^{ps} = \dot{\epsilon}_r^{ps}$ leads to

$$\frac{\partial}{\partial r}(r^2 \dot{\epsilon}_r^{ps}) = 0$$

where the added superscript s denotes the stationary state. Integration of the above with respect to r gives

$$\dot{\epsilon}_r^{ps} = -\sqrt{3}\, K/2r^2 \quad , \quad \dot{\epsilon}^{ps} = K/r^2 \tag{B.1}$$

where K is a positive constant to be determined later. Assuming that the function ϕ in (1.3) is invertible and denoting the inverse by ϕ^{-1}, it follows from (1.3) that

$$\sigma^s = \sigma^{*s}\phi^{-1}[\dot{\epsilon}^{ps}(\sigma^{*s}/G)^{-m}\, \frac{1}{f}\exp(z/RT)] \tag{B.2}$$

Substitution of (B.1) into the above gives

$$\sigma^s = \sigma^{*s}\phi^{-1}[Kr^{-2}(\sigma^{*s}/G)^{-m}\, \frac{1}{f}\exp(z/RT)] \tag{B.3}$$

Using the above and (3.14), the equilibrium equation (3.4) can be written as

$$\frac{\partial \sigma_r^s}{\partial r} - \frac{2}{\sqrt{3}}\frac{1}{r}\,\sigma^{*s}\phi^{-1}[Kr^{-2}(\sigma^{*s}/G)^{-m}\, \frac{1}{f}\exp(z/RT)] = 0$$

Integration of the above with respect to r toegther with (3.16) gives

$$\sigma_r^s(r) = \frac{2}{\sqrt{3}} \int_a^r \frac{\sigma^{*s}}{\eta} \phi^{-1}[K\eta^{-2}(\sigma^{*s}/G)^{-m} \frac{1}{f}\exp(z/RT)]d\eta - p \qquad (B.4)$$

The unknown constant K can be determined by imposing the second of the boundary conditions (3.16). This gives the equation

$$\frac{2}{\sqrt{3}} \int_a^b \frac{\sigma^{*s}}{\eta} \phi^{-1}[K\eta^{-2}(\sigma^{*s}/G)^{-m} \frac{1}{f}\exp(z/RT)]d\eta - p + q = 0 \qquad (B.5)$$

The above equation can be solved for K by some numerical procedure such as the Newton-Raphson method. The equations (3.14) and (B.3) gives the following expression for σ_θ^s;

$$\sigma_\theta^s(r) = \frac{2}{\sqrt{3}} \sigma^{*s}\phi^{-1}[Kr^{-2}(\sigma^{*s}/G)^{-m} \frac{1}{f}\exp(z/RT)] + \sigma_r^s(r) \qquad (B.6)$$

Introducing the following additional nondimensionalized variables

$$\bar{\sigma}_r^s = \sigma_r^s/p \ , \ \bar{\sigma}_\theta^s = \sigma_\theta^s/p \ , \ \bar{\sigma}_z^s = \sigma_z^s/p \ , \ \bar{\sigma}^s = \sigma^s/p \qquad (B.7)$$

the equations (B.5), (B.4) and (B.6) can be written respectively in the forms

$$\frac{2}{\sqrt{3}} \int_1^\kappa \frac{\bar{\sigma}^{*s}}{\eta} \phi^{-1}[\bar{K}\eta^{-2}(\bar{\sigma}^{*s}/\bar{G})^{-m} \frac{1}{f}\exp(z/RT)]d\eta - 1 + \bar{q} = 0 \qquad (B.8)$$

$$\bar{\sigma}_r^s(\xi) = \frac{2}{\sqrt{3}} \int_1^\xi \frac{\bar{\sigma}^{*s}}{\eta} \phi^{-1}[\bar{K}\eta^{-2}(\bar{\sigma}^{*s}/\bar{G})^{-m} \frac{1}{f}\exp(z/RT)]d\eta - 1 \qquad (B.9)$$

and

$$\bar{\sigma}_\theta^s(\xi) = \frac{2}{\sqrt{3}} \bar{\sigma}^{*s}\phi^{-1}[\bar{K}\eta^{-2}(\bar{\sigma}^{*s}/\bar{G})^{-m} \frac{1}{f}\exp(z/RT)] + \bar{\sigma}_r^s(\xi) \qquad (B.10)$$

where $\bar{K} = Ka^{-2}$. Thus, to determine the stationary state of stresses,

first the equation (B.8) is solved numerically for $\bar{K}$. Then the stresses $\bar{\sigma}_r^s(\xi)$ and $\bar{\sigma}_\theta^s(\xi)$ are obtained from the equations (B.9) and (B.10) respectively. The stress $\bar{\sigma}_z^s(\xi)$ is given by the expression

$$\bar{\sigma}_z^s(\xi) = [\bar{\sigma}_r^s(\xi)+\bar{\sigma}_\theta^s(\xi)]/2 \tag{B.11}$$

For 1100 Aluminum alloy we realized from (5.1) that

$$\sigma^s = \sigma^{*s}\exp[-(\dot{\epsilon}^{ps})^{-\lambda}(\sigma^{*s}/D)^{m\lambda}] \tag{B.12}$$

Using the above along with the nondimensionalization (B.7), the equations (B.8)-(B.10) can be written as

$$\frac{2}{\sqrt{3}}\int_1^\kappa \frac{\bar{\sigma}^{*s}}{\eta}\exp[-\bar{K}^{-\lambda}\eta^{2\lambda}(\bar{\sigma}^{*s}/\bar{D})^{m\lambda}]d\eta - 1 + \bar{q} = 0 \tag{B.13}$$

$$\bar{\sigma}_r^s(\xi) = \frac{2}{\sqrt{3}}\int_1^\xi \frac{\bar{\sigma}^{*s}}{\eta}\exp[-\bar{K}^{-\lambda}\eta^{2\lambda}(\bar{\sigma}^{*s}/\bar{D})^{m\lambda}]d\eta - 1 \tag{B.14}$$

$$\bar{\sigma}_\theta^s(\xi) = \frac{2}{\sqrt{3}}\bar{\sigma}^{*s}[-\bar{K}^{-\lambda}\xi^{2\lambda}(\bar{\sigma}^{*s}/\bar{D})^{m\lambda}] + \bar{\sigma}_r^s(\xi) \tag{B.15}$$

For the special case where $\bar{\sigma}^{*s}$ is uniform, the above equations reduce to the following simplified forms:

$$\frac{1}{\sqrt{3}}\frac{\bar{\sigma}^{*s}}{\lambda}[E_1(K^*)-E_1(\kappa^{2\lambda}K^*)] - 1 + \bar{q} = 0 \tag{B.16}$$

$$\bar{\sigma}_r^s(\xi) = \frac{1}{\sqrt{3}}\frac{\bar{\sigma}^{*s}}{\lambda}[E_1(K^*)-E_1(\xi^{2\lambda}K^*)] - 1 \tag{B.17}$$

$$\bar{\sigma}_\theta^s(\xi) = \frac{2}{\sqrt{3}}\bar{\sigma}^{*s}\exp[-\xi^{2\lambda}K^*] + \bar{\sigma}_r^s(\xi) \tag{B.18}$$

where $K^* = \bar{K}^{-\lambda}(\bar{\sigma}^{*s}/\bar{D})^{m\lambda}$ and $E_1(\omega)$ is the exponential integral defined as

$$E_1(\omega) = \int_{\omega}^{\infty} \frac{\exp(-\eta)}{\eta}\, d\eta \qquad (B.19)$$

REFERENCES

[1] Y.N. RABOTNOV. Creep Problems in Structural Members, North-Holland, Amsterdam (1969).

[2] R.K. PENNY and D.L. MARRIOTT. Design for Creep, McGraw-Hill, London (1971).

[3] E. KREMPL. The Interaction of rate and history-dependent effects and its significance for slow cyclic inelastic analysis at elevated temperatures, Nucl. Eng. Des. 29, 125-134 (1974).

[4] E. KREMPL. Cyclic creep-An interpretive literature survey, Welding Research Council Bulletin 195, 63-123 (1974).

[5] E.T. ONAT and F. FARDSHISHEH. Representation of creep of metals, Oak Ridge National Laboratory Report-4783 (1972).

[6] E.W. HART. A phenomenological theory for plastic deformation of polycrystalline metals, Acta Met. 18, 599-610 (1970).

[7] E.W. HART, C.-Y. LI, H. YAMADA and G.L. WIRE. Phenomenological theory: A guide to constitutive relations and fundamental deformation properties, in "Constitutive Equations in Plasticity" (edited by A. ARGON), MIT Press, Cambridge (to appear).

[8] D. LEE and E.W. HART. Stress relaxation and mechanical behavior of metals, Met. Trans. 2, 1245-1248 (1971).

[9] E.W. HART and H.D. SOLOMON. Load relaxation studies of polycrystalline high purity aluminum, Acta Met. 21, 295-307 (1973).

[10] H. YAMADA and C.-Y. LI. Stress relaxation and mechanical equation of state in austenitic stainless steel, Met. Trans. 4, 2133-2136 (1973).

[11] H. YAMADA and C.-Y. LI. Stress relaxation and mechanical equation of state in B.C.C. metal, Acta Met. 22, 249-253 (1973).

[12] H. YAMADA and C.-Y. LI. Stress relaxation and mechanical equation of state in nickel and TD nickel, presented at J.E. Dorn Memorial Symposium on "Rate Processes in Plastic Deformation", Fall Meeting, ASM (1972).

[13] G.L. WIRE, H. YAMADA and C.-Y. LI. Grain boundary sliding and mechanical equation of state in lead, Acta Met., 22, 505-512 (1974).

[14] G.L. WIRE, F.V. ELLIS and C.-Y. LI. Work hardening and mechanical equation of state in some metals in monotonic loading, Acta Met. (to appear).

[15] F.V. ELLIS, G.L. WIRE and C.-Y. LI. Mechanical properties and mechanical equation of state of 1100 Aluminum alloy in monotonic loading, AEC Report No. COO-2172-5, Cornell University, Ithaca, New York (1974).

[16] V. KUMAR and S. MUKHERJEE. Creep of a thick-walled spherical shell: An equation of state approach,ERDA Report No. COO-2733-1, Cornell University, Ithaca, New York (1975).

[17] A.E. JOHNSON, J. HENDERSON and B. KHAN. Behavior of metallic thick-walled cylindrical vessels or tubes subject to high internal or external pressures at elevated temperatures , Proc. Inst. Mech. Engrs. 175, No. 25, 1043-1072 (1961).

[18] E.M. SMITH. Primary creep behavior of thick tubes, Proc. Inst. Mech. Engrs. 178, Pt. 3L, 135-141 (1963-64).

[19] S. TAIRA, R. KOTERAZAWA and R. OHTANI. Creep of thick-walled cylinders under internal pressure at elevated temperatures, Proc. 8th Japan Congress Test. Mat., 53-60 (1965).

[20] S. TAIRA and R. OHTANI. Creep of tubular specimens under combined stress, in "Advances in Creep Design (edited by A.J. SMITH and A.M. NICOLSON), Applied Science, London (1971).

[21] G. SIMMON and H. WANG. Single crystal elastic constants and calculated aggregate properties, MIT Press, London (1971).

FIGURE CAPTIONS

Figure 1. Thick-walled cylinder with closed ends subjected to internal pressure.

Figure 2. Variation of $\bar{\sigma}_r$ with ξ and t for $p = 1250$ psi, $T = 250°$ C and two hardness levels: $\bar{\sigma}_o^*(\xi)=8.493$ (i.e. 10% cold work) and $\bar{\sigma}_o^*(\xi)=3.464$ (i.e. $1.5\,\bar{\sigma}(1,0)$).

Figure 3. Variation of $\bar{\sigma}_\theta$ with ξ and t for $p = 1250$ psi, $T = 250°$ C and the hardness levels $\bar{\sigma}_o^*(\xi) = 8.493$ and $\bar{\sigma}_o^*(\xi) = 3.464$.

Figure 4. Variation of $\bar{\sigma}_z$ with ξ and t for $p = 1250$ psi, $T = 250°$ C and the hardness levels $\bar{\sigma}_o^*(\xi) = 8.493$ and $\bar{\sigma}_o^*(\xi) = 3.464$.

Figure 5. Growth of hardness with time for $p = 1250$ psi, $T = 250°$ C and variable initial hardness $\bar{\sigma}_o^*(\xi) = 1.5\bar{\sigma}(\xi,0)$.

Figure 6. Radial displacement at the inner radius, $u(1,t)$, plotted as function of time at 250° C for the cases:

(I) $p = 2000$ psi, $\bar{\sigma}_o^*(\xi) = 5.308$ (i.e. 10% cold work),

(II) $p = 1250$ psi, $\bar{\sigma}_o^*(\xi) = 1.5\bar{\sigma}(\xi,0)$,

(III) $p = 1250$ psi, $\bar{\sigma}_o^*(\xi) = 2.771$ (i.e. $1.2\bar{\sigma}(1,0)$),

(IV) $p = 1250$ psi, $\bar{\sigma}_o^*(\xi) = 3.464$ (i.e. $1.5\bar{\sigma}(1.0)$)

(V) $p = 1250$ psi, $\bar{\sigma}_o^*(\xi) = 8.493$ (i.e. 10% cold work)

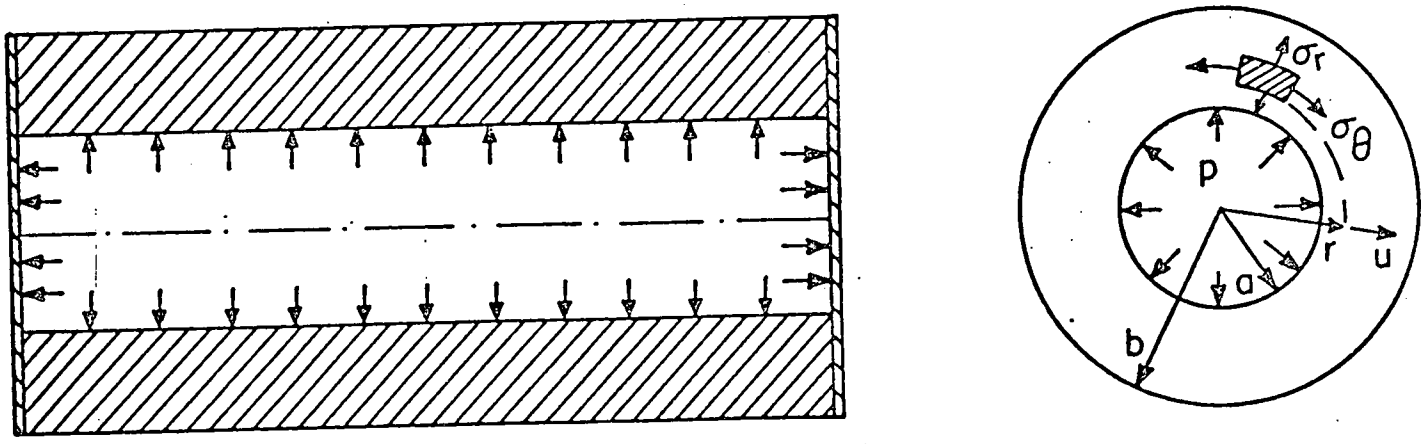

Figure 1. Thick-walled cylinder with closed ends subjected to internal pressure.

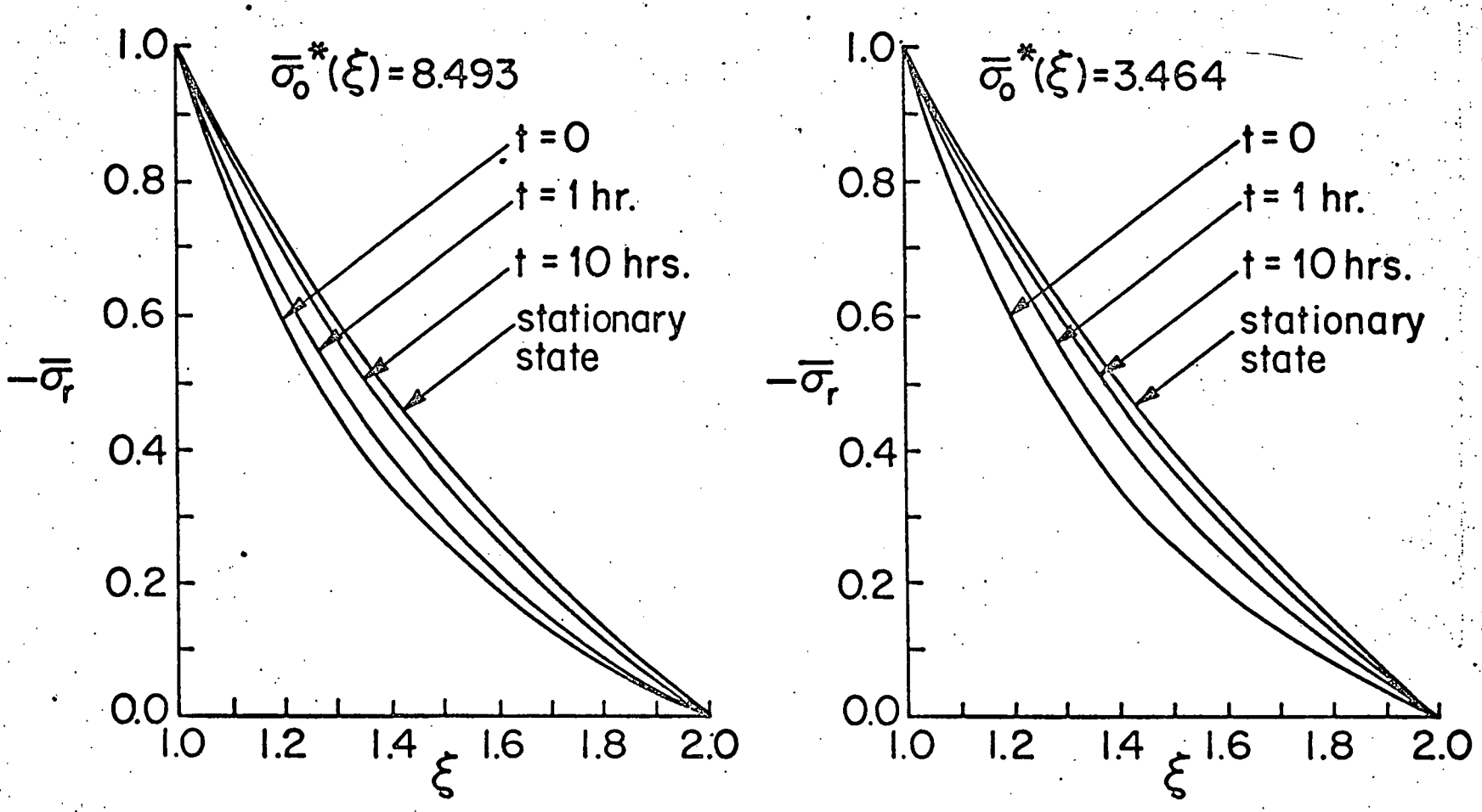

Figure 2. Variation of $\bar{\sigma}_r$ with ξ and t for p = 1250 psi, T = 250° C and two hardness levels: $\bar{\sigma}_o^*(\xi) = 8.493$ (i.e. 10% cold work) and $\bar{\sigma}_o^*(\xi) = 3.464$ (i.e. $1.5\bar{\sigma}(1,0)$).

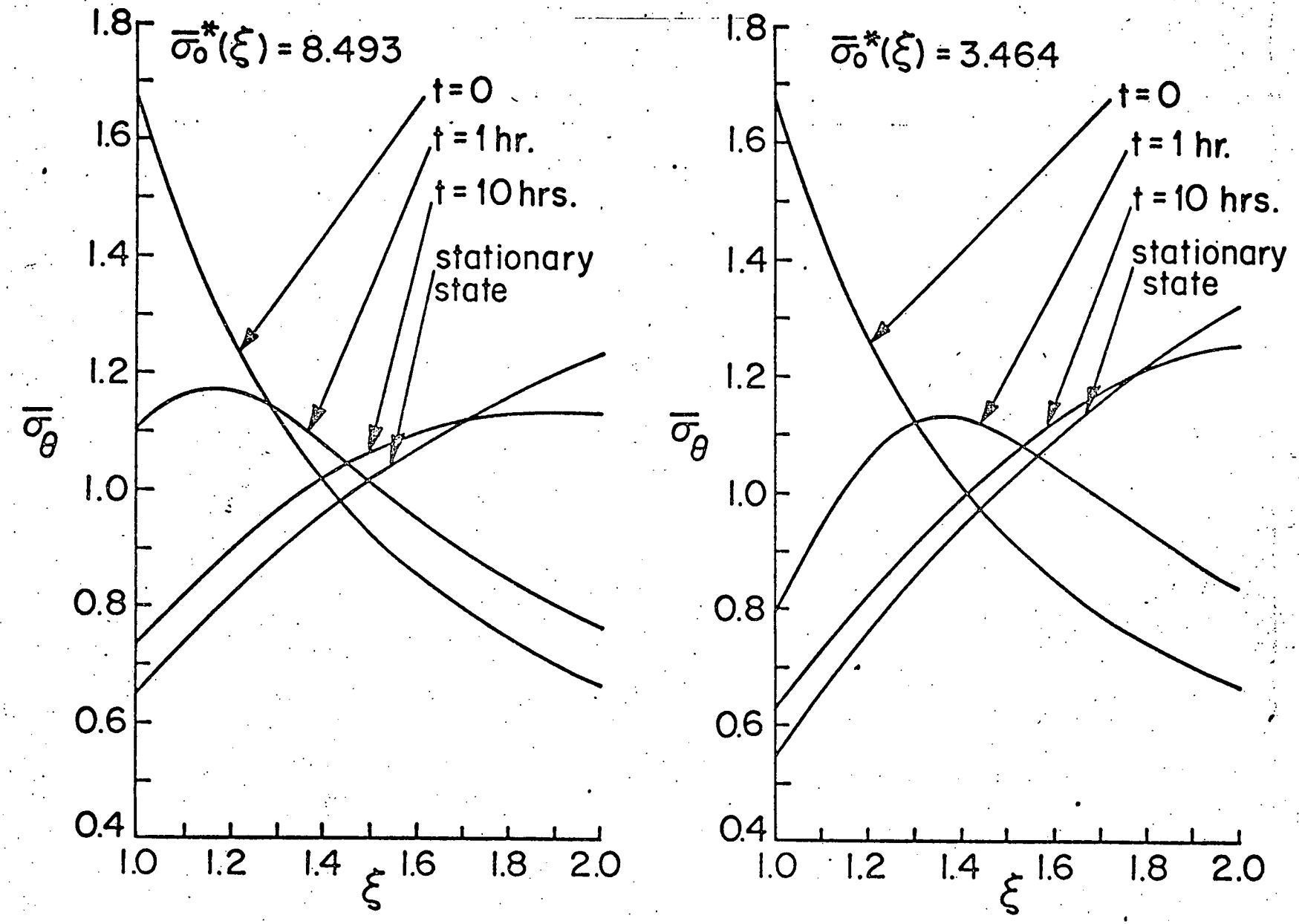

Figure 3. Variation of $\bar{\sigma}_\theta$ with ξ and t for p = 1250 psi, T = 250° C and the hardness levels: $\bar{\sigma}_o^*(\xi) = 8.493$ and $\bar{\sigma}_o^*(\xi) = 3.464$.

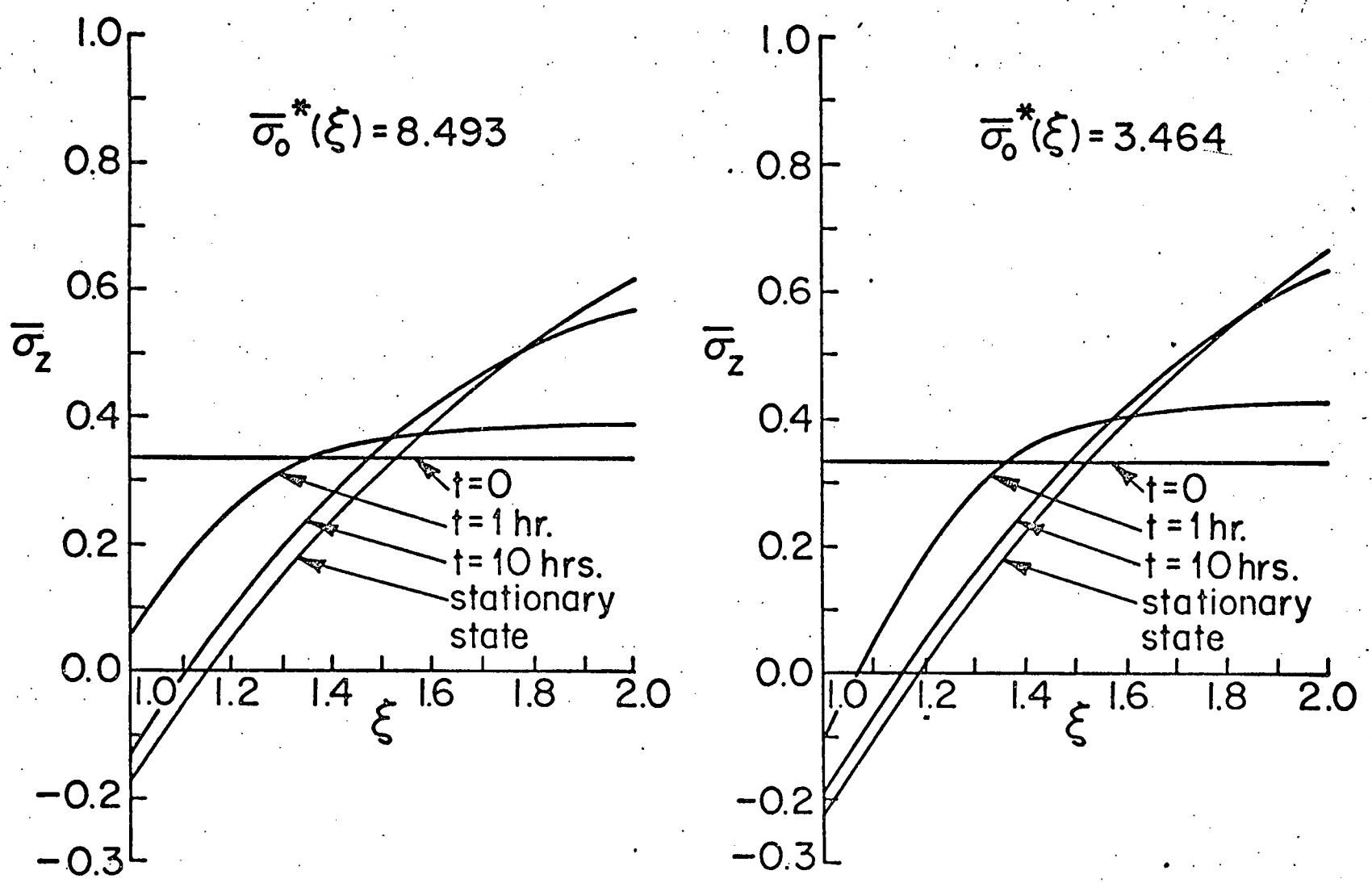

Figure 4. Variation of $\bar{\sigma}_z$ with ξ and t for p = 1250 psi, T = 250° C and the hardness levels: $\bar{\sigma}_o^*(\xi) = 8.493$ and $\bar{\sigma}_o^*(\xi) = 3.464$.

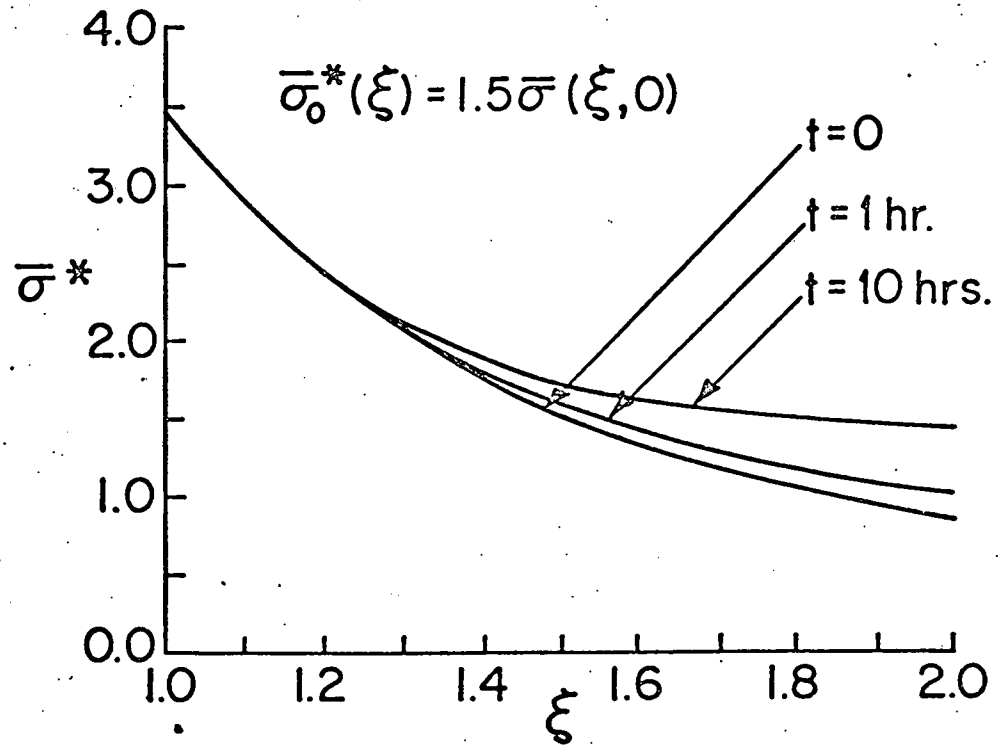

Figure 5. Growth of hardness with time for p = 1250 psi, T = 250° C and variable initial hardness $\bar{\sigma}_o^*(\xi) = 1.5\bar{\sigma}(\xi,0)$.

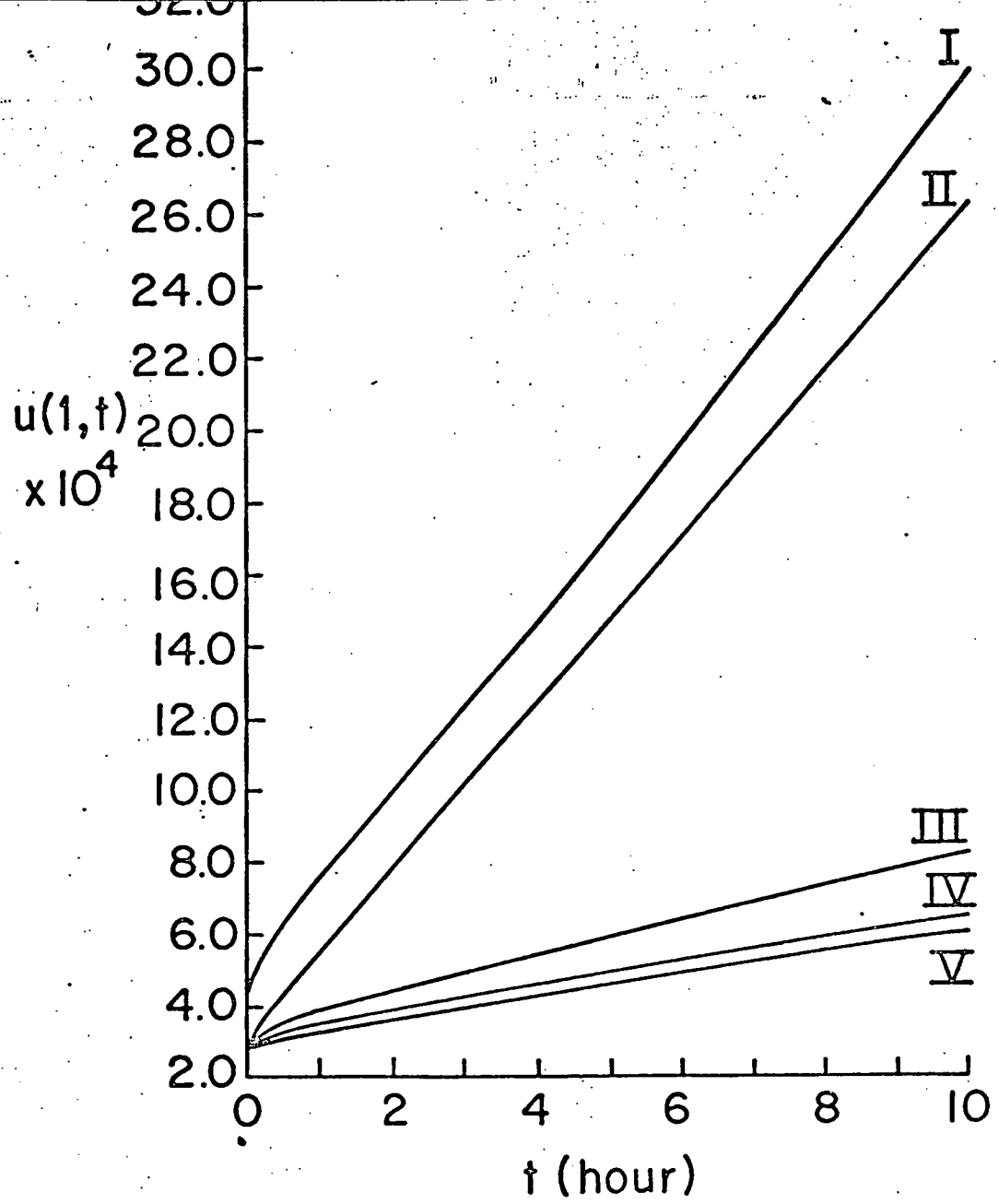

Figure 6. Radial displacement at the inner radius, u(1,t) plotted as function of time at 250° C for the cases:

(I) p = 2000 psi, $\bar{\sigma}_o^*(\xi) = 5.308$ (i.e. 10% cold work),

(II) p = 1250 psi, $\bar{\sigma}_o^*(\xi) = 1.5\bar{\sigma}(\xi,0)$,

(III) p = 1250 psi, $\bar{\sigma}_o^*(\xi) = 2.771$ (i.e. $1.2\bar{\sigma}(1,0)$),

(IV) p = 1250 psi, $\bar{\sigma}_o^*(\xi) = 3.464$ (i.e $1.5\bar{\sigma}(1.0)$)

(V) p = 1250 psi, $\bar{\sigma}_o^*(\xi) = 8.493$ (i.e. 10% cold work)